

Mediterranean flash flood transfer through karstic area

Vincent Bailly-Comte · Hervé Jourde ·
Axel Roesch · Séverin Pistre

Received: 10 November 2006 / Accepted: 1 May 2007 / Published online: 20 June 2007
© Springer-Verlag 2007

Abstract Karstic aquifers influence flash floods propagation in Mediterranean countries. Near Montpellier, Southern France, discharge data are recorded on the Couzou River upstream and downstream of the Aumelas Causse. Two gauging stations are used to describe the hydrodynamics of this binary karstic system. The first station characterizes the non-karstic catchment area. The second one is representative of the karstic part of the watershed. Records since April 2004 are used to understand how the river interacts with a karstic aquifer. Hydrograph analysis of three flash flood events is described. Corresponding discharge time series recorded at the two gauging stations are used to describe the modification of the hydrographs by auto- and crosscorrelations analyses. Finally, linear system analyses are used to provide the transfer functions of this binary karstic system according to the three flood events characteristics (initial conditions, volume, spatial distribution of rainfall, etc.). These functions summarize the hydrodynamic behaviour of the system: their shapes are indicative of the dynamics of the storage, the release and the contribution to surface waters.

Keywords Karst · Flash flood · Fourier transforms · Time-series analysis · Southern France

Introduction

Flood wave propagation of ephemeral rivers through karstic watersheds occurs in several Mediterranean countries. Due to the high permeability of karstic drainage networks, water resources in karstic aquifers are highly sensible to superficial pollution. In the case of binary karstic system with often polluted surface waters, the relationships between the river and the aquifer has to be quantified and operational solutions proposed to manage the water resource. In the South of France, the population is steadily increases, especially near important cities like Montpellier and during the tourist season. Rapid development of urban areas implies significant modifications of land use. Small cities are now spread over areas vulnerable to flood events. Mediterranean countries are characterized by a contrasted climate with very intense rainfall events. Small catchment areas may generate destructive flash-floods in ephemeral river stream beds (Camasara and Segura 2001). Binary karstic aquifers are quite widespread around the Mediterranean basin and these karstic systems are well developed. The local karstic aquifer genesis is related to general geology and to important eustatic variations responsible for high variations of the karstification base-level, especially during the salinity Messinian crisis (Clauzon 1982).

In a binary karstic system characterized by an important allogenic recharge, the surface waters are captured partly or entirely by sinkholes, travel through conduits in the aquifer and eventually discharge through estavelles¹ into the river (resurgence). A general water-table rise within the karst aquifer may induce a significant contribution to

V. Bailly-Comte (✉) · H. Jourde · A. Roesch ·
S. Pistre
Hydrosciences Laboratory, UMR 5569,
University of Montpellier 2,
34095 Montpellier, France
e-mail: bailly@msem.univ-montp2.fr

¹ An estavelle is a karst opening which acts as a sinkhole or as a discharge spring according to the hydrological conditions.

surface waters. For the Coulazou River watershed, previous results indicate initial karstic aquifer recharge followed by significant contribution to surface waters (Jourde et al. 2007).

The main study objective was to understand how the river interacts with the karstic aquifer after intense rainfall events and to propose a methodology which can be applied to other binary karstic systems. Dynamics of the karst storage, release and contribution to surface waters was examined. A release of water through an estavelle refers to previous captured waters in the stream bed; whereas, a contribution is related to a discharge in an estavelle caused by a general water-table rise in the karstic aquifer. This rise is induced by rainfall on the whole karstic catchment area.

Many works document relationships between a river and an aquifer, the bank-storage process. Stream aquifer interactions and movement of bank storage between an aquifer and a river have been extensively studied using analytical solutions (Cooper and Rorabaugh 1963; Pinder and Sauer 1971; Whiting and Pomeranets 1977; Hunt 1990). More recently, some authors have proposed analytical solutions using linear system methods for various boundary conditions (Barlow et al. 2000; Moench and Barlow 2000; Hantush 2005). These studies are devoted to homogeneous aquifers: there is no solution and no method for a fractured and/or a karstic aquifer. Due to the complex geometry of a karstic drainage network it is still difficult even today to propose analytical solutions or a physically based model for such aquifers. The present study focuses on field data: discharge time series are assimilated to signals and signal processing methods are used.

Methodology

The flood wave modification due to karstic storage, release or contribution is considered by the discharge signals modification occurring within the karstic watershed. This method is devoted to binary karstic systems where a flood wave is generated in an upstream non-karstic watershed and reaches a karstic watershed. Upstream and downstream of this karstic watershed, two gauging stations are necessary to describe the hydrodynamics of the system: a first gauging station (G1) characterizes the upstream non-karstic watershed; and a second (G2) is representative of the downstream karstic watershed. Between the two gauging stations, a hydrosystem including the karstic features and the hydrologic watershed is defined and labelled S (Fig. 1).

Flash-flood events are selected and their hydrographs analyzed. Climatic and hydrologic parameters are considered: the spatial distribution and the cumulated values of

the rainfall which generates the flood, the flood duration, the peak discharge, the recession coefficient and finally the runoff volume. From G1 to G2 the evolution of these hydrologic parameters gives information about the influence of the karstic aquifer.

The shape of the hydrographs is described by auto and crosscorrelations analyses. The autocorrelation function is calculated from a biased and normalized estimator (Jenkins and Watts 1968) using Eq. 1. For a given N -length time series, this estimation is correct while the time lag k is between $-N/3$ and $N/3$ (Mangin 1984). The latter interval and the 5 min time step define the observation window.

$$r_{xx_k} = \frac{1}{N \cdot \text{var}(x)} \sum_{t=1}^{N-k} (x_t - \bar{x})(x_{t+k} - \bar{x}) \quad (1)$$

with k the time lag and N , $\text{var}(x)$ and \bar{x} the length, the variance and the time average of the x time series.

By using a $1/N$ instead of a $1/(N-k)$ factor, this biased formulation has some interesting statistical properties, like the decrease of coincidence effects when the time lag k rises. The plot of this autocorrelation function versus the time lag k is called a simple correlogram. It quantifies the linear dependency of successive values over a time period (Larocque et al. 1998). A low decrease of the autocorrelation function characterizes inertial processes. In hydrology, a memory effect arbitrarily corresponds to the time lag k when the autocorrelation function reaches 0.2 (Mangin 1984).

The autocorrelation function calculated with the upstream discharge time series (G1) is compared on the same graph with that calculated with the downstream discharge time series (G2) using the same observation window. For each flood event, the slopes of the two simple correlograms computed upstream (G1) and downstream (G2) are compared. This method allows understanding the flood wave modification for a given time lag. The differences of slopes are interpreted as storage, release or contribution to surface flows within the hydrosystem.

The crosscorrelation function is used in signal processing to represent the energy exchanges of a dynamic system between its entrance and its exit. In the case of a pure random input signal, the crosscorrelation gives the shape of the impulse response of a linear system. The plot of this crosscorrelation function versus the time lag k is called crosscorrelogram. This function describes the response of the hydrosystem: a high decrease characterizes a short term process with low release by the system, and the maximum value gives the transit time of the information (discharge evolution) contained in the time series. The crosscorrelation function is not symmetrical and its estimation is split into two steps. Equation 2 gives the normalized crosscorrelation estimator (Jenkins and Watts 1968; Mangin 1984).

$$\begin{cases} \text{For } 0 \leq k \leq \frac{N}{3} : r_{xyk} = \frac{1}{N \cdot \sqrt{\text{var}(x) \cdot \text{var}(y)}} \sum_{t=1}^{N-k} (x_t - \bar{x})(y_{t+k} - \bar{y}) \\ \text{For } -\frac{N}{3} \leq k \leq 0, \text{ with } k' = -k : r_{yxk} = \frac{1}{N \cdot \sqrt{\text{var}(x) \cdot \text{var}(y)}} \sum_{t=1}^{N-k'} (y_t - \bar{y})(x_{t+k'} - \bar{x}) \end{cases} \quad (2)$$

with k the time lag and N , $\text{var}(x)$, $\text{var}(y)$, \bar{x} and \bar{y} the length, the variance and the time average of the x and y time series.

The negative part of the crosscorrelogram gives information about the time structure of the two signals and the nature of the relationships between the input and the output. Non-zero values in the negative part of the crosscorrelogram are due to a non-random input time-series or to a non-causal system. A peak in the negative part may be indicative of a periodical structure in the input signal. A symmetrical crosscorrelogram highlights that both the input and the output discharge signals react to a third independent signal, precipitation for example (Larocque et al. 1998).

The input signal of the hydrosystem S corresponds to a discharge time series of a flood event. It is a deterministic and time-dependant signal. The shape of the crosscorrelogram cannot be used to obtain the impulse response of the hydrosystem. It is still possible, however, to estimate the average transit time.

Linear system analyses are used to provide the impulse response of this binary karstic system according to the flood events characteristics (initial conditions, volume, spatial distribution of the rainfall, etc.). The transfer operator which transforms the upstream discharge signal (G_1) into the downstream discharge signal (G_2) is expressed as a convolution filter by the following convolution model (Eq. 3). It is assumed that the impulse response of

the system S is the kernel function of the convolution integral.

$$G_2(t) = \int_{\tau=0}^t h(t - \tau) \cdot G_1(\tau) d\tau \quad (3)$$

with h the kernel function, G_1 and G_2 the upstream and downstream discharge time series.

A method based on a convolution model needs to define a system which at least verifies the two following assumptions: the linearity and the time-invariant assumptions. The linearity assumption requires that a unique kernel function is able to describe the whole response of the system, whatever the amplitude of the input. The time-invariant assumption requires that this kernel function does not change with time and is the same all along the hydrological cycle. As a result, seasonal effects are not considered. However, the behaviour of karstic systems is partly related to infiltration processes through the soil and the vadose zone (seasonal effect responsible for time variant processes) and to threshold mechanisms according to the activation of upper preferential pathways. These lead sometimes to overflow discharges, non-linear responses according to the intensity of the event. The previous assumptions are not verified along the hydrological cycle. When a convolution model is applied to a karstic system as a simulation model, several kernel functions have to be proposed according to the intensity of the event. The non-linear processes are replaced by a succession of linear processes, but time variant processes like the infiltration and the transit of water in the vadose zone are not taken into account. However, the objective of this study is to describe the dynamics of the hydrosystem in case of intense flash-floods. Kernel functions are estimated at the time scale of one flood event. For each event, according to hydrogeological conditions, one convolution model with one kernel function is proposed. The method consists in the calculation and the comparison of different kernel functions according to the season, the intensity of the flood event, the spatial distribution of the rainfall, etc. The differences between these functions highlight the differences in the system behaviour according to system input and seasons (time response, losses within the hydrosystem, gain

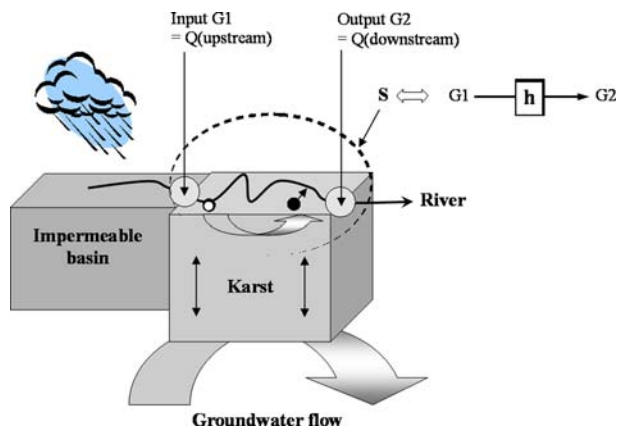


Fig. 1 Definition of the hydrosystem S

by release, etc.). Finally, a convolution model can only be used at this time scale if the initial base-flow before the flood is negligible. If not, a hydrographic separation between the initial base-flows and the quick runoff has to be previously realized. This step is useless in case of flash-floods in an ephemeral river.

From a mathematical point of view, the selected pairs of hydrographs (G1, G2) are used to compute the system kernel functions by the deconvolution method using Fourier transform. It is obvious that the discharge in G2 does not explain the discharge in G1. The system S is a causal system and its kernel function is non-anticipative: $h(t) = 0$ for $t < 0$. In the frequencies domain, the temporal convolution corresponds to a simple multiplication for each frequency. Let $F_{G1(f)}$ and $F_{G2(f)}$ the discrete Fourier transforms of G1(t) and G2(t). The frequency response $H(f)$ is thus determined by the ratio $F_{G2(f)}/F_{G1(f)}$. Finally, the inverse discrete Fourier transform of $H(f)$ gives the kernel function $h(t)$. A kernel function is computed for each selected flash-flood event.

Case study

Monitoring network

Near Montpellier, Southern France the Coulazou River goes through the Aumelas Causse karstic system. Two stations gauge the discharge upstream (G1) and downstream (G2) of the karstic aquifer (Fig. 2). Unfortunately the position of the G1 station, which has to be representative of the system entrance, is not ideal. This station does not consider the significant runoffs occurring in a thalweg on the right side of the Coulazou River, a few meters downstream of the station. Runoff volume at the entrance of the hydrosystem is underestimated. However, the shape of the hydrograph in G1 is assumed to be representative of the system entrance.

The spatial distribution of the rainfall is provided by four rain gauges distributed over the catchment area of the Coulazou River. To describe precisely the relationships between the river and the karstic aquifer, a 5 min time step for all records has been chosen. For the two gauging stations and for such water levels, the confidence interval of the two stage-discharge relationships is about 30%.

Climatic, geological and hydrological settings

The upstream Oligocene watershed and the downstream Jurassic karstic watershed of the river were separately studied (Fig. 2).

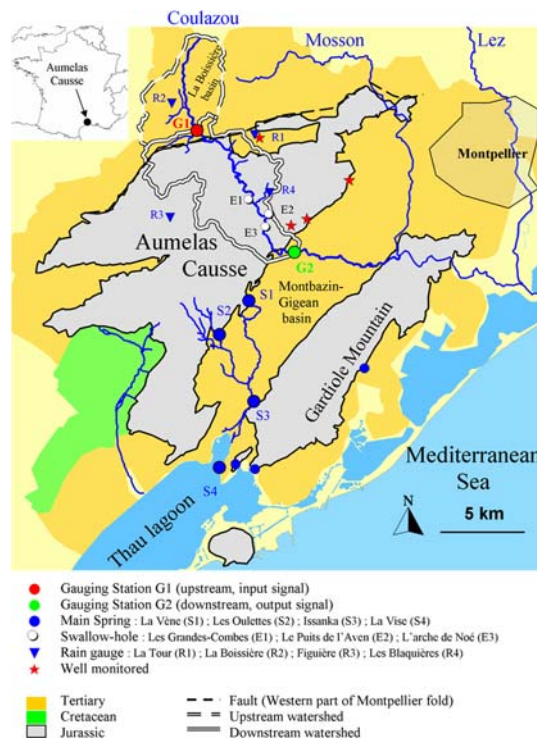


Fig. 2 The study area

- The upstream watershed is a synclinal mainly constituted of marly limestones covered by detritics terrains, with limestone pebbles embedded in a clayey matrix. Its surface is about 20 km². The G1 gauging station is the outlet of this watershed.
- The downstream watershed corresponds to the catchment area on the karstic Jurassic plateau of the Aumelas Causse crossed by the Coulazou River. The surface of this downstream watershed is about 40 km². The G2 gauging station is the outlet of the two continuous watersheds, i.e., the outlet of the hydrosystem S as defined in Fig. 1.

This karstic aquifer plunges to the southwest under the Montbazin-Gigean Miocene basin. Its north boundary corresponds to a major fault where the limestones are in contact with the upstream watershed. The confluence of different small tributaries which start in the upstream watershed gives rise to the Coulazou River. On this impervious upstream watershed, intense Mediterranean rainfalls generate flash-floods. Cumulated rainfall values in 1 day can reach more than 200 mm, as in September 2005. These high rainfall processes are due to powerful convective cells over a limited area. At the hydrosystem outlet (Fig. 1, G2) extreme peak discharges can reach 100 m³/s.

Over 15 main karstic features acting as estavelles have been described along the 10 km long stream bed which crosses the karstic aquifer. These openings realize a direct

and fast stream-aquifer interaction (Bourier 2001). During low flow conditions, the karstic aquifer is drained by the S3 spring used for water supply and by the S4 submarine spring (Bonnet and Paloc 1969). During high flow conditions, two overflow springs (S1 and S2) may have significant discharge. Tracer tests have shown a direct connection with the stream bed of the river.

System identification

This study focuses on the structure of the discharge time series at the system entrance (G1) and the exit (G2) of the karstic system. The two watersheds (Fig. 2) are analysed in accordance with the definition of the hydrosystem S (Fig. 1). The upstream watershed corresponds to the impermeable basin, while the downstream watershed corresponds to the karstic watershed (Fig. 1).

The hydrosystem S is equivalent to the upper part of the karstic aquifer directly connected to the stream bed. A few meters below the surface a more permeable infiltration zone with preferential pathways is assumed to transmit water as a single phase during rapid and intense recharge events (Mangin 1975; Bourier 2001). In this case it is possible to define a dynamic hydrosystem within the karstic aquifer (S, Fig. 1). However, this hydrosystem is only isolated if no other inputs intervene between G1 and G2. General water-level rising or runoffs due to rainfall on the downstream watershed are not taken into account. The hydrosystem S is thus totally defined in terms of space (stream bed geometry and karstic drainage network between G1 and G2), in terms of time scale (the length of the event with a 5 min time interval) and in terms of event intensity (flash flood).

Results

Hydrograph description

Since April 2004, two types of floods have been recorded. A first group corresponds to flood events generated by low to moderate rainfalls. A significant runoff can be observed in the upstream watershed. All the surface waters are captured as the river reaches the karstic terrain. The discharge data recorded in G2 corresponds to the surrounding surface and subsurface runoff processes in the nearest thalwegs. The flow is thus not continuous in the stream bed and a cause-and-effect relationship like the correlation analysis between G1 and G2 does not make sense. The presented method cannot be applied with these events. A second group of floods is related to extreme rain events. As long as the runoff is greater than the infiltration rate, the flood wave spreads itself and reaches the G2 station. In that case the study of a cause-and-effect relationship between G1 and G2 is relevant to understand the stream-karstic drainage network relationships. Generally, the water-level in the estavelles is insufficient to observe a discharge. The general water-table of the karstic aquifer rises and overflows in S1 and S2. But during an extreme flood event, as in December 2002, some estavelles in the stream bed may discharge water with a flow rate greater than several tens m³/s (Fig. 1, E2).

Fifteen floods have been recorded, but three only belong to the second group. Characteristics of these events are presented in Table 1. Numerous methods have been used for base-flow separation of runoff and subsurface flows, but a straight-line method seems to be the easiest and probably no more arbitrary than other methods (Dreiss 1983). The

Table 1 Results of the hydrographs study. All data have a 5 min time step

Date (TU)	Flood 1	Flood 2	Flood 3
Beginning	29 april 2004 12h25	6 oct. 2004 23h35	6 sept. 2005 06h40
End	5 may 2004 15h25	8 oct.2004 08h00	10 sept.2005 17h35
Rainfall on the upstream watershed (R2)	85, 20 mm	140 mm	230 and 85 mm
Rainfall on the downstream watershed (mean of R1, R3 and R4)	60 and 20 mm	30 mm	120 and 90 mm
Input G1			
Quick runoff duration	12h40	04h30	07h00 and 07h45
Total volume (Vtot ₁)	322,000 m ³	150,000 m ³	411,000 m ³
Recession coefficient (α)	1 day ⁻¹	4 day ⁻¹	3 and 1.5 day ⁻¹
Peak discharge (Qmax ₁)	5.2 m ³ /s	12.4 m ³ /s	17.2 and 6.6 m ³ /s
Output G2			
Quick runoff duration	14h00	02h45	03h40 and 12h25
Total volume (Vtot ₂)	1,670,000 m ³	176,000 m ³	1,940,000 m ³
Recession coefficient (α)	0.7 day ⁻¹	10 day ⁻¹	10 and 1 day ⁻¹
Peak discharge (Qmax ₂)	29.0 m ³ /s	19.0 m ³ /s	110.0 and 38.0 m ³ /s

recession period is delimited and estimated by a linear fit in a semi-logarithmic plot. Figure 3 shows the hydrographs separation method used to estimate the recession coefficient. Figure 4a, b, c present the selected pairs of hydrographs (G1, G2).

These floods are very different in term of generated rainfalls, runoff duration, recession coefficient etc., but they all characterize a flash flood. After the surface runoff peak has passed, the hydrograph follows a groundwater based depletion curve. Following a flash-flood event, percolation to groundwater induces base flow characterized by the recession coefficient (Fig. 3, Table 1). This coefficient is indicative of water release in the stream bed.

Correlations analyses

Considering the fast response time and the very low inertia of the hydrosystem, a 24 h (288 time lags) or 12 h (144 time lags) observation window with a 5 min time step is well adapted to study the time structure of these flash-floods. Figure 5a, b, c present the resulted auto- and crosscorrelation function computed with the three pairs of hydrographs.

Interpretation

For the first flood, a periodic structure is remarkable in G1 (Fig. 4a, G1). It corresponds to the peak at the time lag 56 (4h40) in Fig. 5a. For a time lag between 72 and 144 (6 and 12 h, respectively), the shape of the autocorrelation function describes the transition between the quick flows and the base flow. After the time lag 144 (12 h) the autocorrelation function does not change anymore; the flood energy is totally dissipated. This stable part is related to the recession period where the discharge is no longer influenced by quick flows. The end of the quick-flows and the beginning of the recession period in G1 is estimated at 12h40 (Table 1). Downstream the periodic structure is less obvious because of a change of amplitude (Fig. 4a, G2). A

damping on the autocorrelation function appears for a time lag about 56 (Fig. 5a, G2). The two peaks of discharge are thus routed without phase lags. This observation is in accordance with the linearity assumption. For higher time lags, the same conclusion about the transition between the quick flows and the base flow can be given. The change of amplitude (Fig. 3a, G2) is partly due to the spatial distribution of rainfall. Runoff in thalwegs within the Aumelas Causse was significant and caused a higher memory effect, since the autocorrelation function is greater in G2 than in G1 (Fig. 5a). Due to this spatial distribution of rainfall, the hydrosystem S is not isolated. The low value of the recession coefficient (Table 1, $\alpha = 1 \text{ day}^{-1}$ in G1, $\alpha = 0.7 \text{ day}^{-1}$ in G1) is indicative of a significant contribution to surface flows. For the flood 1, the relationships between the river and the aquifer are characterized by a general water-table rising in the whole aquifer, which leads to an increase of flood inertia within the hydrosystem. For this event, Jourde et al. (2007) have shown by modelling

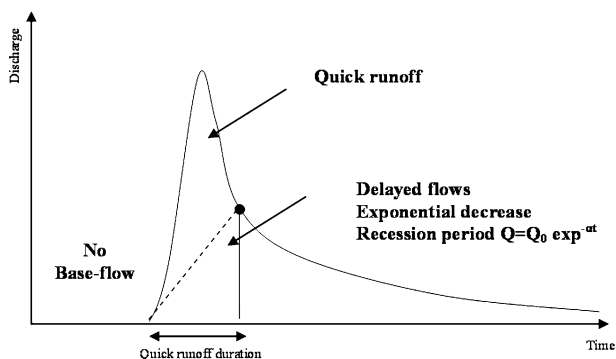


Fig. 3 Hydrograph separation

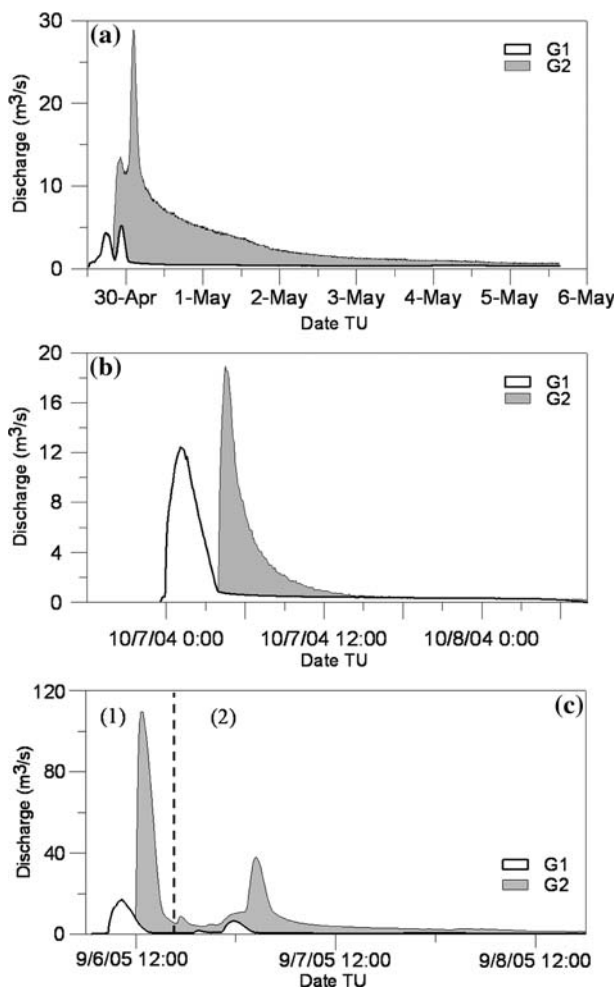


Fig. 4 a Flash-flood event 1. b Flash-flood event 2. c Flash-flood event 3

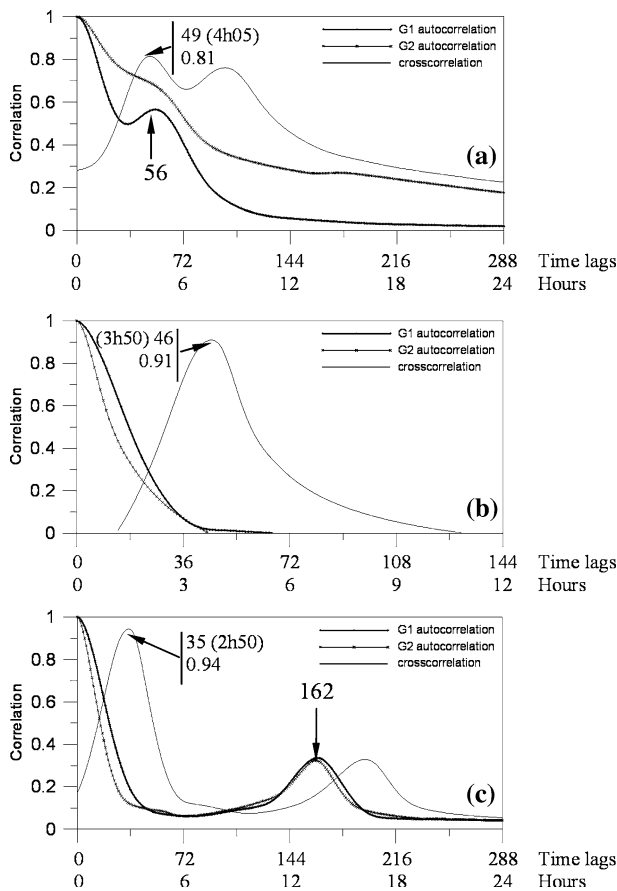


Fig. 5 **a** Autocorrelation functions and crosscorrelation function computed with the flood 1. **b** Autocorrelation functions and crosscorrelation function computed with the flood 2. **c** Autocorrelation functions and crosscorrelation function computed with the flood 3

that the contribution to surface waters reaches 30% of the total volume recorded in G2. This contribution induces a greater base-flow component in G2.

For the second flood event (Fig. 5b) the two autocorrelation functions are almost identical. The temporal structure of the flood wave is conserved. The fast decrease of these correlograms indicates a very low inertia behaviour in accordance with the high values of the estimated recession coefficient (Table 1, $\alpha = 4 \text{ day}^{-1}$ in G1, $\alpha = 10 \text{ day}^{-1}$ in G2). This inertia is lower in G2 than in G1. The shape of the autocorrelation function in G2 shows a faster decrease of the flood energy than in G1. The hydrosystem modifies the flood wave by decreasing its inertia. The peak flow in G2 is sharper and the hydrosystem has partly stored the surface waters and has modified the shape of the flash-flood just after the peak discharge. In Fig. 5b and in Table 1, the volume and the peak discharge are slightly greater in G2 than in G1. Considering the inaccuracy of the stage-discharge relationships and the underestimation of the input of the hydrosystem, storage within the hydrosystem may occur even if the volume in G2 is higher than

the volume in G1 (Table 1). Discharge in G2 is increased by the rainfall (30 mm in Table 1), which has induced some runoffs in small thalwegs.

The autocorrelations functions of the third flood event present two main peaks (Fig. 5c). They are related to a flood event which can be split into two parts (Fig. 3c). About 13h30 separates the two maxima. The first one is due to an upstream located rainfall, while the second one is due to a more homogeneous rainfall (Table 1). The autocorrelation function is sensitive to such periodical processes. For this reason a second maximum of autocorrelation is remarkable at the time lag 162 (13h30) in Fig. 3c. This periodic structure is clearly visible and identical in G1 and in G2. The temporal structure of the flood wave is well conserved without phase lags. This is once more in accordance with the linearity assumption. The first parts of the two autocorrelation functions (for time lag less than 72) are fairly equivalent to the autocorrelation functions obtained with the flood event 2. The same conclusion can be given: the stronger decrease of the autocorrelation function in G2 than in G1 is again related to the storage of the surface waters.

The analysis of the autocorrelation functions and of the spatial rainfall distribution leads to several conclusions. For flood 1, the runoff is partly controlled by the whole aquifer. The contribution of the saturated zone of the aquifer is effective. For the flood 1 and the second part of the flood 3, the rainfall on the karstic watershed has to be taken into account. For the flood 2, the hydrosystem S can be considered as a single-input/single-output system (SISO system) only controlled by the input in G1 and the output in G2.

The crosscorrelation analysis shows that the transit time of the hydrosystem varies between 2h50 and 4h05 (Fig. 5a, b, c). The maximum of the crosscorrelation function is noticeably lower for flood 1 (0.81 vs. 0.91 and 0.95 for flood 1, 2 and 3, respectively). The downstream discharge recorded during the flood 1 cannot be explained only by the upstream discharge. Groundwater contribution is significant. This process is longer than a simple runoff process and may elongate the transit time.

The negative parts of the crosscorrelation function are not represented in Fig. 5. Nevertheless, for floods 1 and 3, this negative part presents non-zero values which are indicative of periodical inputs. This is the reason why the two corresponding simple correlograms present two maxima in Fig. 5a, c. For flood 2, the negative part can be neglected. The crosscorrelogram in Fig. 5b gives a good representation of the exchange of energy between the entrance and the exit of the hydrosystem, and shows how the hydrosystem S store and release the energy of the flood wave. The observation window is well chosen and all the information contained in the time series (discharge evolution) is transferred through

the hydrosystem *S* in less than 12 h. A 12-h observation window is sufficient to estimate the three corresponding kernels functions of the hydrosystem *S*.

Convolution model and kernel function estimation

The flood event 1 and the second peak of the flood event 3 may not be ideal to study the hydrosystem *S* because of significant rainfall on the karstic watershed (Table 1). Therefore, only the first part of the flood 3 has been used to compute the kernel function (part 1, Fig. 3c). Flood 1 is also used to analyze the method sensitivity. The results are plotted on Fig. 6a, b, c.

For the second flood event (Fig. 6b), two characteristic times can be given. The transit time corresponds to the time lag of the first non-zero value. It is estimated at 45 time steps (3h45). This result is in accordance with the analyses of the crosscorrelation functions. The response time is the time lag which corresponds to the maximum of the kernel function. This is estimated to 50 time steps (4h10). A sharp peak is remarkable on the graph. This peak is followed by a fast decrease with negative values between the time lags 54

and 63 (4h30 and 5h15, respectively). This change of positives values into negatives values is indicative of the flood energy storage, i.e., the storage of a volume of surface waters in the karstic drainage network. A low positive response is related to the delayed flows. The high frequencies of oscillations can be due to a slight failure to respect the time-invariant assumption which is not completely verified during the 12 h, as well as some noise in the times series.

For the third flood, only the first part of the event has been used (Fig. 3c). A transit time of about 3h10 and a response time of 3h20 are obtained. This transit time is higher than that estimated by the crosscorrelation function using the whole event. In the second part of this event, the rainfall on the downstream watershed is responsible for an underestimated transit time by the crosscorrelation analysis. The period corresponding to a storage process in flood 1 is less important. A significant peak can be observed between time lags 45 and 54 (3h45 and 4h30, respectively). This peak is attributed to the release of water from the karstic drainage network to the surface waters.

For the first flood event, the method is maladapted and oscillations are stronger than the response of the hydro-system. Previous studies dealing with the deconvolution have considered these strong oscillations were due to a method extremely sensitive to minor errors in the input-output data (Long and Derickson 1999). In this study, these oscillations seem to be caused by the system. If the system is not isolated, the convolution does not make sense. The error comes from the method which does not consider the rainfall over the downstream watershed and the general rise of the water level. As a result, downstream discharge variations are not linearly dependent on the upstream discharge variations, and an isolated system as described in Fig. 1 is inappropriate.

Discussion

The correlation analyses at the time scale of a flood event allows expressing the correlation function as the energy contained in the time series (autocorrelation) or exchanged through the hydrosystem (crosscorrelation). These analyses give information about the modification of the flood wave within the hydrosystem. As these functions are normalized, only the shape of the hydrograph is analyzed and the change in amplitude is not considered. Contrary to a comparison of the total of the runoff volume upstream and downstream of the karstic watershed, the correlation analyses are less influenced by an under- or overestimation of the discharge time series.

Concerning the kernel function estimation and the convolution model, this study shows that linear system

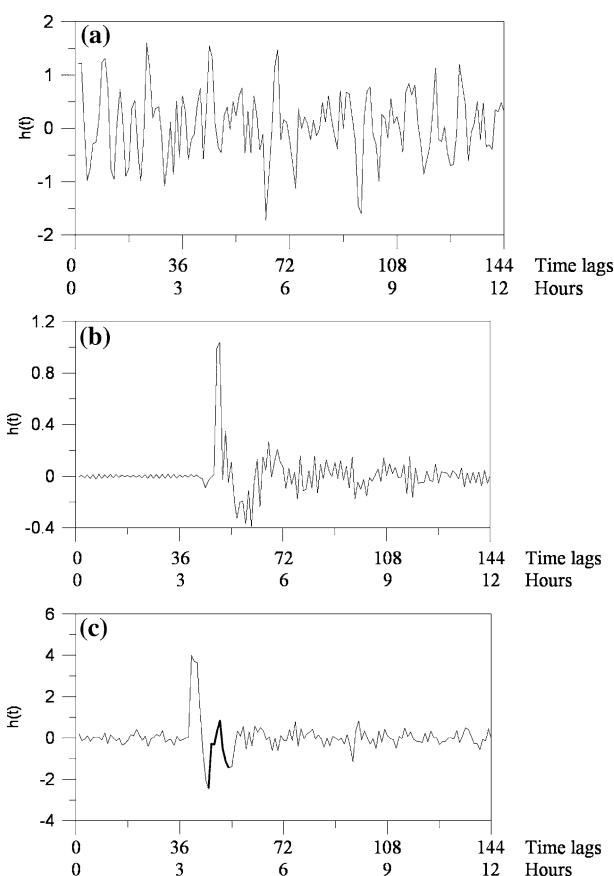


Fig. 6 **a** Kernel function computed with the flood 1. **b** Kernel function computed with the flood 2. **c** Kernel function computed with the flood 3

methods can be used to characterize a binary karstic system. The shape and the order of magnitude of these kernel functions are different, however. This indicates that the hydrosystem S is time-variant at a higher time scale. The deconvolution method cannot be used at a larger time scale. The kernel function estimation is very sensitive to the boundary conditions of the hydrosystem S. In particular, the influence of additional input plays a prominent part on the efficiency of these estimations. A precise descriptive approach has to precede the application of the deconvolution method. Thanks to the rainfall monitoring, it can be assumed for flood 3 that the second peak of the kernel function corresponds to the contribution of the karstic drainage network to the surface waters (Fig. 6c). Without a good knowledge of the spatial rainfall distribution it is not possible to distinguish a karstic contribution from another time shift runoff in other thalwegs. The hydrosystem S acted as a loss for flood 2.

The kernel functions allow these three different hydrodynamic behaviours to be described. Differences do not clearly appear by the correlation analysis. The crosscorrelation functions are often used to describe the transfer operator of a black-box system which transforms a rain signal into a discharge signal. For a transformation of a discharge signal into another discharge signal, crosscorrelation analysis may lead to mistaken conclusions. Errors come from the use of a discharge time series as input of the system: contrary to a rainfall time series, a discharge time series can not be used as a random signal at the time scale of a flood event. The trend in a discharge series could have been removed using a differential filter, but the results would have been too much sensitive to low variations and to the noise in the time series. However, the transit time estimated by the crosscorrelation function or by the kernel function are of the same order of magnitude.

Conclusion

For each flash flood event, the relationships between the river and the karstic drainage network has been described by different approaches. The correlations analyses have shown the dynamics of the storage in the karstic drainage network. The kernel function estimation shows that significant contribution to surface waters can be attributed to the passage of waters through the karstic drainage network and their discharge through estavelles. For the flood 3, the modification of the flash-flood wave is directly related to the previous captured waters in the stream bed. This is a storage/release process. For the flood 2, the kernel function highlights the storage capacity of the karstic drainage network. Finally, for the flood 1 the general rise of the water level in the whole karstic aquifer

is responsible for a significant contribution which cannot be determined by the analysis of the kernel function. For this event, the autocorrelation functions show how the energy of the flood increases thanks to the karstic aquifer contribution to surface flows. These three flash-flood events characterize three different behaviours of the hydrosystem and the presented method shows how the hydrosystem reacts to the different inputs. Although, the case study of the Coulazou River leads to select only intense flood events (flash-flood), the study method is useful for other systems. This study can more generally be applied to all binary karstic systems for different intensity of floods and for different spatial scale, but the time scale of the flood event is required.

Acknowledgments The authors acknowledge M. Grevellec and M. Ruas from the “Conseil Général de l’Hérault”, M. Debaille and M. Coustol from the “Syndicat intercommunal d’adduction d’eau du Bas Languedoc”, M. Hernandez from the HydroSciences Laboratory and the helpful comments provided by R. Bourier of the SpeleoClub of Cournonterral.

References

- Barlow PM, DeSimone LA, Moench AF (2000) Aquifer response to stream-stage and recharge variations. II. Convolution method and applications. *J Hydrol* 230(3–4):211–229
- Bonnet A, Paloc H (1969) Les eaux des calcaires jurassiques du bassin de Montbazin-Gigean et de ses bordures (Pli de Montpellier et massif de la Gardiole, Hérault). *BRGM* 2(3):1–12
- Bourier R (2001) Observations du fonctionnement du Coulazou aussi bien en surface que sous terre. *Speleoclub of Cournonterral, SCC—34660 Cournonterral, France*
- Camarasa Belmonte AM, Segura Beltrán F (2001) Flood events in Mediterranean ephemeral streams (ramblas) in Valencia region, Spain. *Catena* 45(3):229–249
- Clauzon G (1982) Le canyon messinien du Rhône: une preuve décisive du “dessicated-deep model” (Hsü, Cita et Ryan, 1973). (The Rhone river Messinian canyon: a definite demonstration of the “dessicated-deep model”). *Bull Soc Géol Fr* 24(7):597–610
- Cooper HH, Rorabaugh MI (1963) Ground-water movements and bank storage due to flood stages in surface streams. *Geological survey water-supply paper 1536-J*. United States government printing office, Washington
- Dreiss SJ (1983) Linear unit-response functions as indicators of recharge areas for large karst springs. *J Hydrol* 61(1–3):34–44
- Hantush MM (2005) Modeling stream-aquifer interactions with linear response functions. *J Hydrol* 311(1–4):59–79
- Hunt B (1990) An approximation for the bank storage effect. *Water Resour Res* 26(11):2769–2775
- Jenkins GM, Watts DG (1968) *Spectral analyses and its applications*. Holden-Day, San Francisco, 525 p
- Jourde H, Roesch A, Guinot V, Bailly-Comte V (2007) Dynamics and contribution of karst groundwater to surface flow during Mediterranean flood. *Environ Geol* 51:725–730
- Larocque M, Mangin A, Razack M, Banton O (1998) Contribution of correlation and spectral analyses to regional study of a large karst aquifer (Charentes, France). *J Hydrol* 205(3–4):217–231
- Long AJ, Derickson RG (1999) Linear systems analyses in a karst aquifer. *J Hydrol* 219(3–4):206–217

- Mangin A (1975) Contribution à l'étude hydrodynamique des aquifères karstiques. Thèse de Doctorat ès Sciences, Université de Dijon, 124 p
- Mangin A (1984) Pour une meilleure connaissance des systèmes hydrologiques à partir des analyses corrélatoire et spectrale. *J Hydrol* 67(1–4):25–43
- Moench AF, Barlow PM (2000) Aquifer response to stream-stage and recharge variations. I Analytical step-response functions. *J Hydrol* 230(3–4):192–210
- Pinder GF, Sauer SP (1971) Numerical simulation of flood wave modification due to bank storage effects. *Water Resour Res* 7(1):63–70
- Whiting PJ, Pomeranets M (1997) A numerical study of bank storage and its contribution to stream flow. *J Hydrol* 202(1–4):121–136